



Measurement-based Detector Characteristics for Digital Twins in aRTist 2

Tamara REUTER^{1*}, Florian WOHLGEMUTH¹, Carsten BELLON², and Tino HAUSOTTE¹

¹Chair of Manufacturing Metrology, Friedrich-Alexander-Universität Erlangen-Nürnberg (FAU), Nägelsbachstraße 25, Erlangen, Germany, e-mail: tamara.reuter@fmt.fau.de, tino.hausotte@fmt.fau.de

²BAM Federal Institute for Materials Research and Testing, Unter den Eichen 87, Berlin, Germany, e-mail: Carsten.Bellon@bam.de

*Contact: tamara.reuter@fmt.fau.de

Abstract

Various software products for the simulation of industrial X-ray radiography have been developed in recent years (e.g., aRTist 2, CIVA CT, Scorpius XLab, SimCT, Wilcore) and their application potential has been shown in numerous works. However, full systematic approaches to characterise a specific CT system for these simulation software products to obtain a truthful digital twin are still missing. In this contribution, we want to present two approaches to obtain realistic grey values in X-ray projections in aRTist 2 simulations based on measured projections. In aRTist 2, the displayed grey value of a pixel is based on the energy density incident on that pixel. The energy density is calculated based on the X-ray tube spectrum, the attenuation between source and detector as well as an energy-dependent sensitivity curve of the detector. The first approach presented in this contribution uses the sensitivity curve as a free modelling parameter. We measured the signal response at different thicknesses of Al EN-AW6082 at different tube voltages (i.e., different tube spectra). We then regarded the grey values displayed by these projections as a data regression respectively an optimisation problem and obtained the sensitivity curve that is best able to reproduce the measured behaviour in aRTist 2. The resulting sensitivity curve does not necessarily hold physical meaning but is able to simulate the real system behaviour in the simulation software.

The second approach presented in this contribution is to estimate the sensitivity curve based on assumptions about the characteristics of the scintillation detector (e.g., scintillator material, scintillator thickness and signal processing characteristics). For this approach, a linear response function (linear relationship between the deposited energy per pixel and the resulting grey value) is assumed. If the detector characteristics, which affect the simulated deposited energy, are properly modelled, the slope and offset of the response function to match the measured grey values should be the same for different tube spectra. As the offset is constant and given by the grey values measured at no incident radiation, the slope is the remaining parameter to evaluate the success of the detector modelling. We therefore adapted the detector characteristics by changing the detector setup until the slope was nearly the same for all measured tube spectra. We are aware that the resulting parameters of the scintillator material and thickness might not be the real ones, but with those modelling parameters we are able to simulate realistic grey values in aRTist 2. Both of those approaches could potentially be a step forward to a full systematic approach for a digital twin of a real CT system in aRTist 2.

Keywords: Computed Tomography, Simulation, Digital Twin

1. Introduction

Various software products for the simulation of X-ray radiography have been developed in recent years (e.g. aRTist [1], CIVA CT [2], Scorpius XLab [3], SimCT [4], Wilcore an Inhouse developed software from Siemens Healthineers) and their application potential has been shown in numerous works (e.g. [5-7]). However, systematic approaches to characterise a specific CT system for this simulation software to obtain a real digital twin are an ongoing research topic [8,9]. First works towards this goal either concern the determination of the acquisition geometry [10,11] or are specifically tailored towards a specific simulation platform [12].



A first work to characterise a scintillation detector is given in [13]. However, none solve the problem of developing a general procedure to build a realistic grey value characteristic and further to model the X-ray detector in aRTist. In this paper, we want to present two approaches to obtain realistic grey values in aRTist simulations based on measured projections. Both approaches could potentially be a building block for a full systematic approach to constructing a digital twin of a real CT system in aRTist.

The first approach is based on the following assumptions. In aRTist, we assume the X-ray tube spectrum to be given by the included spectrum calculator. This spectrum calculator has been shown to achieve realistic results [14-15]. Assume that the spectral density is given by $s(E)$ with E denoting X-ray energy. The spectrum is attenuated by matter according to the Lambert-Beer-law. Supposing we know the measurement setup, the attenuated spectral density $s_{\text{att}}(E)$ can be calculated. In the real measurement setup, the detector shows some grey value GV . In a black-box-approach, we are looking for the mapping from attenuated spectral density to grey value:

$$s_{\text{att}}(E) \mapsto GV \quad (1)$$

In general, this map could be very complex – so even if we sample many data points, it might be difficult to determine that map due to the high degrees of freedom.

In CT simulations, the spectral density is discrete and we know details about the modelling approach. It should be easier to determine this map because both discreteness and modelling approach restrict the possible mappings and thus, the search space.

The second approach is based on the assumption, that most of the used flat panel detectors in industrial computed tomography systems have within a certain range a linear grey value characteristic. With this assumption and the possibility to model realistically the deposited energy per pixel by variation of the detector sensitivity it should be possible to determine the detector characteristics and thus realistic grey values. In aRTist 2 we can simulate a linear response function (linear correlation between deposited energy per pixel and displayed grey values) via the JSON file interface developed in the research project CTSimU. The missing parameters that have to be calculated are the slope and the offset of this function. In order to gain a realistic slope of the above mentioned function, we have to determine the detector sensitivity (e.g., scintillator material, scintillator thickness and signal processing characteristics). The interface allows us to variate this sensitivity by changing the scintillator thickness until a realistic slope is met and thus realistic grey values can be modelled. [16] Consequently, with this approach it is also possible to estimate the scintillator thickness (by known scintillator material).

Chapter 2 describes how we adapt these general ideas for aRTist simulations. Chapter 3 describes the experimental setup and the results on our experimental data. Chapter 4 summarises the results and provides an outlook towards subsequent work.

2. Principles and Methods

2.1 Calculating the detector characteristic curve by the detector signal response

In aRTist, the displayed pixel grey value GV is given by:

$$GV = g(ED) + \frac{g(ED)}{n(ED)} \cdot \mathcal{N}(0,1) \quad (2)$$

Here, ED is the pixel energy density, g the energy dependent grey value characteristic and n the energy dependent noise characteristic. $\mathcal{N}(0,1)$ is a Gaussian random variable. The energy density at the pixel can be calculated as:

$$ED = \frac{I \cdot \Omega \cdot t}{A} \cdot \sum_i \sigma_i \cdot I_i \cdot E_{\text{dep},i} \cdot \exp\left(\int_S -\mu_i(x) dx\right) \quad (3)$$

Here, I is the tube current, Ω is the solid angle of the pixel, t is the exposure time and A is the pixel surface. I_i is the spectral flux in energy bin i with bin energy E_i as calculated by the tube model included in aRTist (see [4]), σ_i is the interaction probability in energy bin i and $E_{\text{dep},i}$ the deposited energy in the detector upon interaction. $\mu_i(x)$ is the energy-dependent attenuation coefficient on the line S connecting source and detector pixel.

Measuring projections with constant and known attenuation $\int_S -\mu_i(x) dx$ (i.e., a specific material in a known geometry) and setting $\sigma_i = 1$ as well as $E_{\text{dep},i} = E_i$, we can construct a grey value characteristic $g(ED)$ in equation (2). This grey value characteristic does however have limited usefulness. Due to the change of the X-ray spectral distribution upon changing voltage or penetrated material, this grey value characteristic can only be used to simulate penetration of the specific material used at the chosen tube voltage and current settings.

To obtain a spectral characteristic that is useable across different voltage and current settings, we need to account for the spectral response of the detector by not simplifying with $\sigma_i = 1$ and $E_{\text{dep},i} = E_i$. A possible approach is to deduct these parameters from the physical properties of the detector parts (e.g. scintillator used). In this first approach, we want to regard the determination of these values as an optimisation problem. We want to find coefficients $w_i \in [0,1]$ such that energy densities calculated with

$$ED = \frac{I \cdot \Omega \cdot t}{A} \cdot \sum_i I_i \cdot w_i \cdot E_i \cdot \exp\left(\int_S -\mu_i(x) dx\right) \quad (4)$$

agree in the sense that measurements with the same grey value also have the same calculated energy density. This energy density can then be used to construct one grey value characteristic $g(ED)$ (equation (2)) valid for all measurements.

For the optimisation, we need an expression to minimise. As discussed in chapter 3, we measured different material thickness (thus, energy density) – grey value curves which we will call ‘characteristics’. We use the sum of squared energy density differences at the same grey value between the different measured grey value characteristics as error function. Let c_1, c_2 be two such characteristics mapping energy density to grey value ($c_i: ED \mapsto GV$). Let Ω_1, Ω_2 be their grey value codomains. The error function Δ is then:

$$\Delta = \int_{\Omega_1 \cap \Omega_2} dGV (c_1^{-1}(GV) - c_2^{-1}(GV))^2 \quad (5)$$

For more than two characteristics, the error function value of all pairs is averaged.

In each iteration, the measured grey value characteristics are updated using the current set of weights w_i for the recalculation of all energy densities and their respective distances, resulting in an updated error function value. The set of weights w_i are optimised by minimising the

error function using the global optimisation of The MathWorks, Inc. MATLAB. As our optimisation changes the weights w_i which influence the error function, we need to rescale our error function such that it remains invariant against reductions of all weights by a common factor (e.g. 0.1). This is achieved by rescaling the error function to the average decimal of all values after each iteration.

2.2 Calculating the detector grey value characteristics by use of a linear response function

With our second approach we are calculating the detector characteristics in aRTist by assuming a linear relationship (see formula (6)) between the collected deposited energy per pixel $E_{\text{dep},px}$ in J and the resulting grey value GV .

$$GV = f \cdot E_{\text{dep},px} + \text{offset} \quad (6)$$

We have to calculate the factor f and the offset within this formula. The offset can be calculated from the mean grey value of the dark images. The “factor”, the slope within this formula, has the inverse unit of $E_{\text{dep},px}$, 1/J. The deposited energy per pixel is dependent on the incoming X-ray spectrum and the detector sensitivity and can be simulated.

We assume now, that if we model the real X-ray spectrum and the detector sensitivity by assuming especially the scintillator material and thickness, we can assign a given real grey value characteristic to the deposited energy per pixel and can calculate afterwards the f . As f is the only missing parameter, we have afterwards the possibility to simulate the detector characteristics.

To solve this formula (6), we need to obtain experimentally many different X-ray spectra by changing the tube current, voltage and the pre-filter. As the grey value characteristic is dependent on the detector response, it is important to generate the experimentally gained projections only with one detector setting, meaning the same integration time and gain. Our assumption is, that we will get a cluster of the different factors of the different tube spectra for one specific scintillator material and thickness with which we have to build our digital twin. The results might not be the real one, but results in the best digital replica of the grey value characteristic of one detector based on the assumption of a linear grey value characteristic. If we have found the scintillator material and thickness, we can calculate for every spectrum f and determine the linear response function to simulate a realistic detector characteristic.

3. Results and discussion

All Measurements have been performed using the Zeiss (Oberkochen, Germany) CT system ‘Metrotom 1500’ at the Chair of Manufacturing Metrology. This system is equipped with a microfocus X-ray tube with a reflection target, and has a source-detector-distance of roughly 1380 mm. We will start presenting the results for the first approach.

3.1 Results and discussion for approach from 2.1

Projections of slabs of aluminium (EN-AW6082, different thicknesses) were taken at 1000 ms exposure time, 16 x gain, without image averaging and without binning. The slabs were positioned close to the X-ray tube as to minimise the effect of scatter by minimising the solid angle of the detector as seen from the aluminium slabs. Four X-ray tube voltage-current settings (100 kV/720 μA , 140 kV/360 μA , 180 kV/180 μA and 200 kV/180 μA) were used with a 0.25 mm Cu filter. In all projections, the aluminium covered the whole projection. The nominal thickness of the aluminium slab is taken as the thickness for the whole projection. Due to the large source-detector-distance, the average thickness error due to the cone beam is below 1 %.

The projections were gain-corrected according to:

$$P_{\text{corr}}(i, j) = \bar{B} \frac{P(i, j) - D(i, j)}{B(i, j) - D(i, j)} \quad (7)$$

Here, B is the bright image, D the dark image and P the uncorrected projection. i and j are the pixel indices and P_{corr} the gain-corrected projection. \bar{B} is the mean of the bright image over all pixels.

For each slab thickness and tube setting, energy densities were calculated according to equation (4), resulting in four characteristic curves of energy density – grey value data. Figure 1 shows the grey value characteristics before and after optimisation. While the characteristics without weights are clearly different and would necessitate multiple detector settings in the simulation platform, the characteristic with weights is able to reproduce all measured values using one single detector configuration. Being able to simulate realistically using different X-ray spectra instead of just a single one is not only convenient but also allows simulating how changes in tube settings will affect image quality.

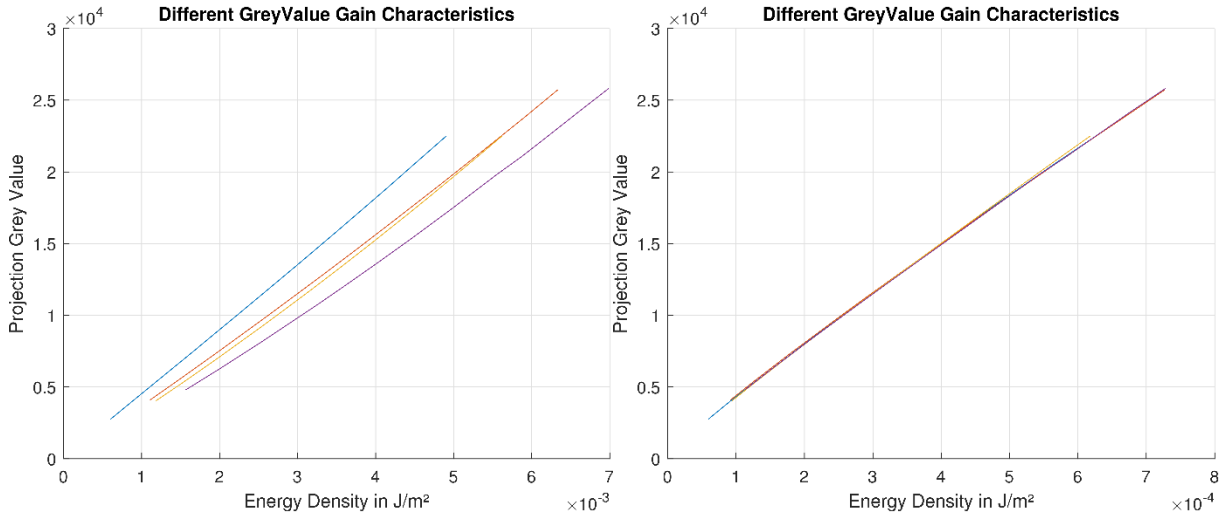


Fig. 1 Left figure: Measured grey values over energy densities calculated according to equation (3) with $\sigma_i = 1$ and $E_{\text{dep},i} = E_i$. The attenuation of the X-ray intensity was achieved with Al EN-AW6082 at different thicknesses as attenuator. Exposure time and tube current were kept constant for each series of measurements. The different acceleration voltages clearly display a different behaviour due to the different spectral distributions of the X-rays at the different acceleration voltages. Right figure: Same measurement data plotted over energy densities calculated according to equation (4) after determination of a set of w_i by optimisation. The detector characteristic with spectral weights is approximately able to reproduce all measurements.

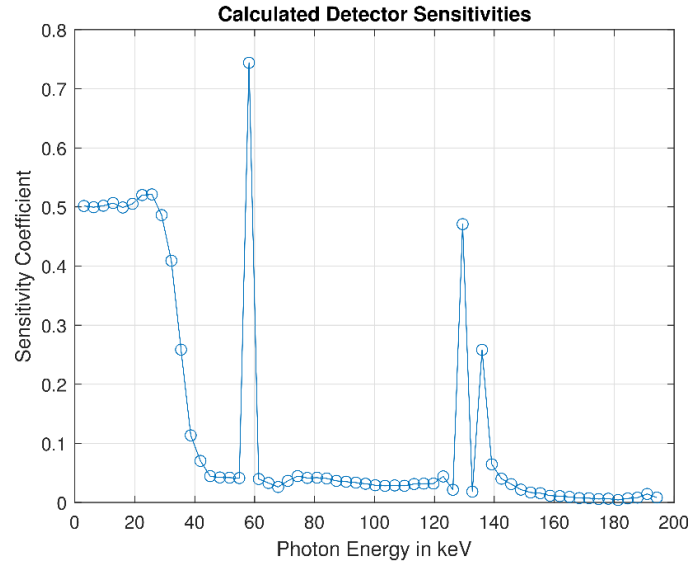


Fig. 2 Set of w_i determined by optimisation.

It is important to note that the set of w_i resulting from the optimisation does not represent any physical property of the detector. It is simply the set of weights that is best able to reproduce the behaviour of the real detector in the simulation platform (under the assumption that the real X-ray tube spectrum is well represented by the calculated X-ray tube spectrum.) As no modelling assumption were made nor any characteristics of the detector taken into account, there is no guarantee that this set of weights describes the physical properties of the detector. Especially, there is no absolute scale included in the weights. Figure 2 shows the set of w_i determined for the data in figure 1.

3.2 Results and discussion for approach from 2.2

For the second approach we acquired for each setting 200 empty projections. The settings differed in tube voltages, 75 kV - 225 kV in 25 kV-steps and currents, 100 μ A - 1300 μ A in 400 μ A-steps. We used as a pre-filter copper with 0.5 mm, 1 mm and 2 mm thicknesses and an integration time of 1000 ms.

Those settings were then simulated with varying detector sensitivities, meaning different thicknesses of the assumed scintillator material, Gadolinium oxysulfide doped with 8 % terbium (further called Gadox), to model the deposited energy per pixel. The factor f for each setting was calculated according to formula (7). To solve this formula, we had to execute an offset correction of the real projections, determine the mean grey value of the projections and divide this mean grey value by the modelled mean deposited energy per pixel. For the offset correction we subtracted the measured grey values by the measured dark field grey values with no radiation.

Fig. 3 shows the results of the different simulated scintillator thicknesses and tube spectra. For comparison reasons, we divided each calculated minimum factor by the calculated maximum factor with constant tube voltage but varying current. If the result is close to one, the resulted f for each spectrum setting must be nearly the same for one specific scintillator thickness and we have found the modelling parameter for the detector. The results in Fig 3 indicate, that at a tube voltage of 100 kV to 225 kV we can model a scintillator thickness of about 200 μ m to 400 μ m.

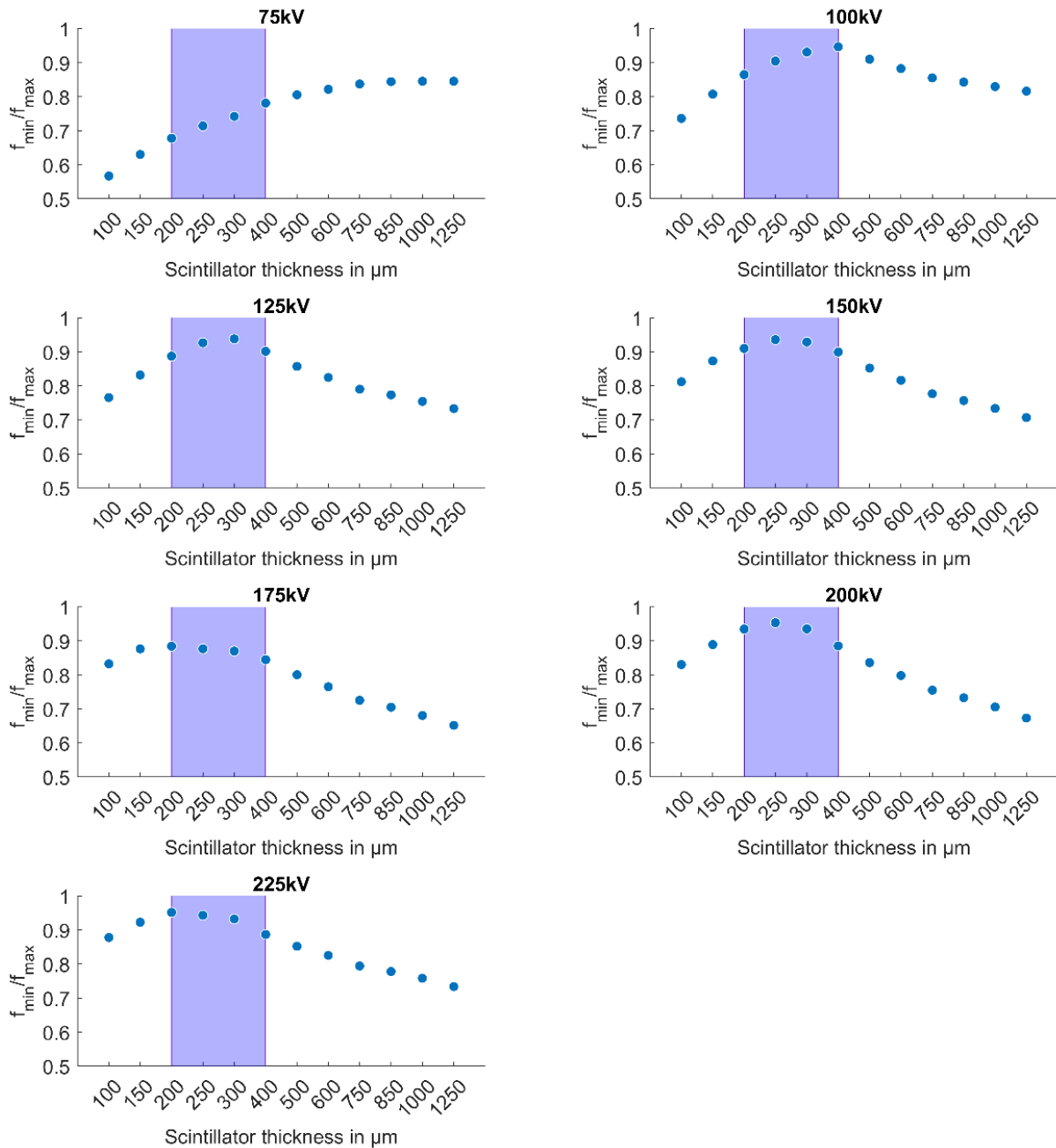


Fig. 3 Calculated ratio of minimal factor and maximal factor with constant tube voltage but varying current in relation to the modelled scintillator thickness. The expected scintillator thickness is marked in purple.

The results, however, give no clear result for one thickness. This can be led back due to too less spectra and thus data points. At a tube voltage of 75 kV we have no distinct maximum at a reasonable scintillator thickness. This might be due to the sensitivity curve of the used material Gadox.

Fig 4 illustrates the sensitivity curve of this material given in aRTist [17]. The curve shows at a given energy in keV the resulting mean deposited energy (keV) in a pixel $E_{\text{dep},px}$ for an incoming photon. It can be seen, that at an energy of about 75 keV a peak exists. This means, that at a given energy of 75 keV the highest deposited energy in pixel for an incoming photon will be produced. In reality, most of the emitted photons at a tube voltage of 75 kV do not have an energy of 75 keV. This could lead to the fact, that the scintillator material is not sensitive

enough for tube voltages below 75 kV. Therefore, the allocation of the simulated $E_{\text{dep},px}$ to real GV give us no clear result for one scintillator thickness. With increasing photon energy, the slope of the sensitivity curve (s. Fig. 4) decreases at about 100 keV and lead to a more stable calculation of the material thickness. Another possible explanation can be the fact, that with 75 kV we had less bright images and we got outliers. This can mislead the results.

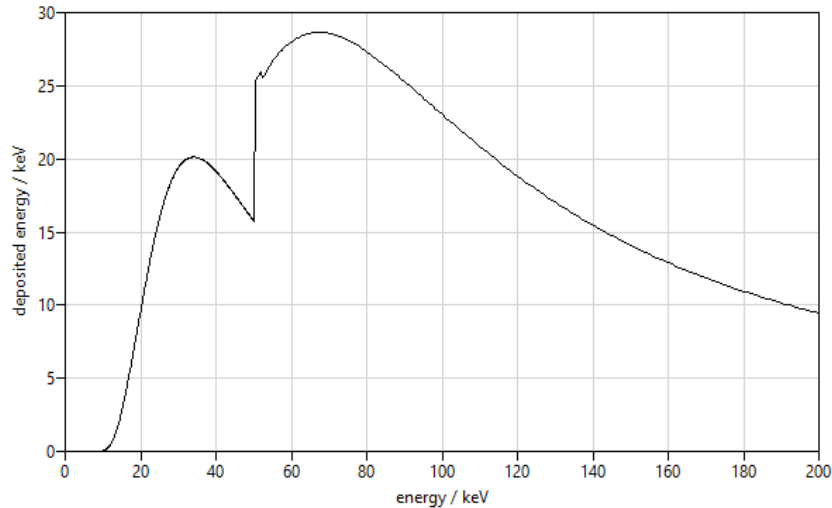


Fig. 4 Sensitivity curve of Gadox derived from aRTist [17]. It shows at a given energy in keV the resulting mean deposited energy (keV) in a pixel $E_{\text{dep},px}$ for an incoming photon.

We compared our results with the scintillator thickness gained with the method described in [13]. The cone beam device presented in [13] enables the calculation of the attenuation curve and the determination of the scintillator thickness. With this method we got also a scintillator thickness between 200 μm and 250 μm which are comparable with our results at tube voltages higher than 125 kV.

4. Conclusions

This contribution presented two independent approaches to model realistic detector characteristics in aRTist. The first approach shows that by optimisation, a suitable detector characteristic for the simulation platform aRTist can be derived from measurements. This approach could be used for any other simulation platform which uses a similar modelling approach. It still needs to be tested which width of different tube settings can be represented by one set of simulation sensitivities and whether multi material measurements are within the scope of the presented approach. Details concerning this approach can also be found in [18].

The second approach shows a possible solution for estimating the scintillator thickness and further realistic grey value characteristics. It presented the usage of the JSON file interface with which it is possible to determine the linear response function of detector. We showed that it is possible to estimate the scintillator thickness by known material for a specific detector. In first studies with different spectra, we generated grey values that are close to realistically gained grey values. Furthermore, we tested this approach in first studies with different tube settings and materials. The attenuation showed good agreement for the used CT system. The approach needs to be tested with different simulation software, CT systems and test specimens to give an idea if it is a general approach to determine the detector characteristics. A possible further study can be the determination of the scintillator thickness by a full optimisation approach similar as presented in approach 1.

Author Contributions according to CRediT Taxonomy [19]

Florian Wohlgemuth (F. W.) contributed Conceptualization, Data curation, Formal Analysis, Investigation, Methodology, Software, Visualization as well as Writing - original draft and Writing – review & editing of the first approach. Tamara Reuter (T. R.) contributed Conceptualization, Data curation, Formal Analysis, Investigation, Methodology, Software, Visualization as well as Writing - original draft and Writing – review & editing of the second approach. Carsten Bellon (C. B.) contributed assistance concerning aRTist 2 implementation and details (Software) as well as Writing - review & editing. Tino Hausotte T. H., F. W. T.R., contributed to Funding acquisition. T. H. contributed Project administration, Resources, Supervision and Writing - review & editing.

Acknowledgement

The first approach of this project (17IND08 AdvanCT) has received funding from the EMPIR programme co-financed by the Participating States and from the European Unions Horizon 2020 research and innovation programme.

The second approach was funded through the project Wipano-CTSimU2 (WIPANO project 03TN0049A). WIPANO projects are financed by the German Federal Ministry for Economic Affairs and Climate Action and managed by Project Management Jülich.

The logo for WIPANO, with the letters W, I, P, A, N, O in a stylized font. The 'I' and 'A' are red, while the others are black. There are thin vertical lines passing through the letters.

Gefördert durch:



Bundesministerium
für Wirtschaft
und Klimaschutz

aufgrund eines Beschlusses
des Deutschen Bundestages

The authors want to thank all partners for the content-related discussions.

The Chair of Manufacturing Metrology would like to thank the German Research Foundation (DFG) for the financial support of the acquisition of the CT system "Zeiss Metrotom 1500" through Grant No. 324672600.

References

- [1] C. Bellon, K. Burger and C. Gollwitzer, “Virtual CT acquisition and reconstruction of complex and noisy scanning trajectories in aRTist”, Proceedings of the 9th Conference on Industrial Computed Tomography, Padova, Italy (2019)
- [2] Extende, “COMPUTED TOMOGRAPHY WITH CIVA”, <http://www.extende.com/computed-tomography-with-civa/> (30 Dec. 2023)
- [3] J. Hiller, T. Fuchs, S. Kasperl and L. Reindl, “Einfluss der Bildqualität röntgentomographischer Abbildungen auf Koordinatenmessungen Grundlagen, Messungen und Simulationen“, Technisches Messen, Vol. 78, pp. 334-347 (2011)
- [4] M. Reiter, M. Erler, C. Kuhn, C. Gusenbauer and J. Kastner, “SimCT: A simulations tool for X-ray imaging”, NDT.net issue, Vol. 21, No. 02, (2016)
- [5] R. Christoph, H. Weise, C. Leinweber and M. Kachelrieß, “Examination of a Method for the Optimization of Scan Parameters for Measuring with Computed Tomography”, Proceedings of the 8th Conference on Industrial Computed Tomography, Wels, Austria (2018)
- [6] P. Fuchs, T. Kröger and C. Garbe, “Self-supervised Learning for Pore Detection in CT-Scans of Cast Aluminum Parts”, Proceedings of the International Symposium on Digital Industrial Radiology and Computed Tomography DIR2019, Fürth, Germany (2019)

- [7] A. Müller, F. Wohlgenuth and T. Hausotte, “Simulation-based correction of systematic errors for CT measurements”, Proceedings of the 8th Conference on Industrial Computed Tomography, Wels, Austria (2018)
- [8] WIPANO CTSimU2, <https://www.ctsimu2.forschung.fau.de> (30 Dec. 2023).
- [9] F. Wohlgenuth, “Digital Twins of Computed Tomography Systems; Contributions to a Systematic Approach”, PhD Thesis, Friedrich-Alexander Universität, Erlangen-Nürnberg (2022)
- [10] M. Ferrucci, “Systematic approach to geometrical calibration of X-ray computed tomography instruments”, PhD Thesis, KU Leuven (2018)
- [11] B. A. Bircher, F. Meli, A. Küng, and R. Thalmann, “CT geometry determination using individual radiographs of calibrated multi-sphere standards”, Proceedings of the 9th Conference on Industrial Computed Tomography, Padova, Italy (2019)
- [12] J. Hiller, “Abschätzung von Unsicherheiten beim dimensionellen Messen mit industrieller Röntgen-Computertomographie durch Simulation”, PhD Thesis, IMTEK, University of Freiburg (2011)
- [13] F. Borges de Oliveira, J. Illema, “Validation of an easy-to-use beam-hardening measurement method” Proceedings of the 12th Conference on Industrial Computed Tomography, Fürth, Germany (2023)
- [14] A. Deresch, “Modellierung von Röntgenspektren für technische Anwendungen”, PhD Thesis, University Potsdam, Germany (2015)
- [15] A. Deresch, C. Bellon and G.-R. Jaenisch, “A general spectrum model for X-ray generators”, NDT & E International, Vol. 79, pp. 92–97 (2016)
- [16] CTSimU Scenario Descriptions 1.2, <<https://bamresearch.github.io/ctsimu-scenarios/>> (30 Dec. 2023)
- [17] aRTist Handbook, <<https://bamresearch.github.io/aRTist-handbook/index.html>> (14 Jan. 2024)
- [18] F. Wohlgenuth, “Digital Twins of Computed Tomography Systems; Contributions to a Systematic Approach”, PhD Thesis, University of Erlangen-Nürnberg, Germany (2022)
- [19] CASRAI, “CRedit”, <<https://credit.niso.org/>> (30 Dec. 2023)